Available online at www.sciencedirect.com
ScienceDirect
Journal of the European Ceramic Society 31 (2011) 313–320
www.elsevier.com/locate/jeurceramsoc

# Fabrication and characterization of sintered TiC–SiC composites

J. Cabrero [a,b,*], F. Audubert [b], R. Pailler [a]

[a] LCTS, University of Bordeaux, 3 Allé de la Boétie, 33600 Pessac, France
[b] CEA/DEN/DEC/SPUA, Cadarache, 13108 Saint Paul lez Durance, France

Received 29 July 2010; received in revised form 23 September 2010; accepted 2 October 2010
Available online 1 November 2010

**Abstract**

Some TiC–SiC composites with different SiC volume contents (0, 10, 25 and 50%) are prepared by spark plasma sintering (SPS). The relationship between density, grain growth and temperature is studied in order to fabricate dense and nano-sized TiC–SiC composites. A sintering by SPS at 1800 °C during 5 min allowed to form TiC–SiC composites with relative density above 95% and an homogeneous distribution of TiC (grain size from 270 to 900 μm) and nano-sized SiC. With the increasing of SiC volume contents, Vickers hardness and fracture toughness are improved; thermal conductivity at room temperature is increased whereas at high temperature it is reduced. In future studies, those materials will be irradiated to characterize monolithic TiC and TiC–SiC composites behaviour under irradiation.
© 2010 Elsevier Ltd. All rights reserved.

*Keywords:* Spark plasma sintering; SiC; TiC; Thermal conductivity; Nuclear applications

## 1. Introduction

Silicon carbide (SiC) presents interesting features with respect to high temperature applications in neutron radiation environment.[1] As monolithic SiC is a brittle ceramic, the structural applications will likely involve SiC fibers-reinforced ceramics.[2] Continuous fibers-reinforced composites provide better thermomechanical properties compared to such monolithic materials. Nevertheless, their radiation behaviour is a key point. Among the present issues, thermal conductivity of $SiC_f$/SiC composites is reduced in high temperature environment, but also in radiation environment.[1,3–5] Thermal conductivity of $SiC_f$/SiC has to be improved to be used as fuel cladding in some next generation fission reactor.

One proposes to act on the intrinsic conductivity of the matrix by introducing more or less large fraction of transition metal carbides. These carbides, because of their metallic bonds, have a real potential for nuclear environment. Titanium carbide (TiC), whose conductivity is partially electronic and increases with temperature is a potential material.[6,7] However, prior to fabricate such fibers-composite, understanding the fundamental mechanisms for radiation damage in monolithic TiC is necessary.

The objective of the present paper is to fabricate TiC and TiC–SiC samples and to determine their mechanical and thermal properties, in order to assess later their behaviour under irradiation and the evolution of the properties. The study was performed on five compounds, pure TiC and SiC, and three TiC–SiC composites with 50 vol.% SiC, 25 vol.% SiC and 10 vol.% SiC. In order to assess only the SiC content effect on composite properties, it is necessary to fabricate ceramics which present similar microstructure (density, grain size). The sintering process selected is spark plasma sintering (SPS) because this set-up enables to fabricate many specimens very fast, with a very fine microstructure. Various studies have already presented the sintering of TiC–SiC composites by SPS, giving sintering conditions and mechanical characterizations,[8–10] but were limited to some ranges of compositions. On the other hand, there is no data about temperature dependence of thermal conductivity of TiC–SiC composites.

## 2. Experimental procedure and characterization

This work was performed by using commercially available nano-powders of TiC ($d$ = 30–80 nm) and β-SiC ($d$ = 45–55 nm) from nanoamor. The compositions with different SiC contents

* Corresponding author at: LCTS, University of Bordeaux, 3 Allé de la Boétie, 33600 Pessac, France.
*E-mail address:* cabrero@lcts.u-bordeaux1.fr (J. Cabrero).

0955-2219/$ – see front matter © 2010 Elsevier Ltd. All rights reserved.
doi:10.1016/j.jeurceramsoc.2010.10.010

Table 1
Sintering conditions.

| | Temperature max (°C) | Heating rate (°C/min) | Pressure from 1000 °C (MPa) | Holding time (min) |
|---|---|---|---|---|
| Run 1 | | | | |
| 1 | 1600 | 100 | 50 | 10 |
| 2 | 1700 | 100 | 50 | 10 |
| 3 | 1800 | 100 | 50 | 10 |
| 4 | 1900 | 100 | 50 | 10 |
| Run 2 | | | | |
| 5 | 1800 | 100 | 75 | 5 |

were mixed by a mortar and pestle with medium of alcohol. Flowing stir-drying at 100 °C for 4 h, the mixture was reground (Retsch MM200, 30 min, 18 Hz). The sintering of SiC–TiC composites with different SiC volume ratio, from 0% to 50%, was studied by SPS at different temperatures, pressures and holding times. In order to select the temperature which leads to samples with fine microstructure and low porosity, pressure and holding time were maintained at 50 MPa for 10 min, whereas temperature ranges from 1600 °C to 1900 °C. Then, other samples were sintered at 1800 °C (the optimized temperature), but with pressure of 75 MPa, and holding time of 5 min. The vapour pressure during sintering was kept below 6 Pa. The different processing conditions for the preparation of SiC–TiC composites are listed in Table 1.

The as-sintered samples were ground to remove the graphite layer and then analyzed by X-ray diffraction (XRD) with Cu Kα radiation at 40 kV and 40 mA, and by scanning electron microscopy (SEM). The density was measured by Archimede's method. The grain size or equivalent disk diameter was calculated using SEM images, with the hypothesis of spherical grains. In order to determine the effective TiC content in the TiC–SiC composites, the surface of the polished materials was also analyzed with an electron probe microanalyser (EPMA, Cameca SX-100) with wavelength-dispersive spectrometer operated at an acceleration voltage of 20 kV, and a probe size of 1 μm in diameter. At least 10 measurements were taken.

hardness of the TiC–SiC composites was measured by using a Vickers diamond indenter and calculated by taking the average of 20 points randomly selected in the composite. The fracture toughness was estimated from indentation technique on the surface of samples by measuring crack length generated by a Vickers indentor. The indentions were made using 20 N load with a dwelling time of 10 s.

The measurement of thermal diffusivity coefficient $\alpha$ was carried out by using a laser flash method at room temperature. Measurements from 400 °C to 1600 °C were also performed with a laser flash apparatus in a flowing $N_2$ atmosphere. The thermal conductivity $\kappa$ was calculated from the relationship $\kappa = \rho\alpha Cp$, where $\rho$ and $Cp$ are respectively the measured density and the estimated specific heat of the composites. The specific heat capacity ($Cp$) of SiC and TiC was evaluated from Snead et al.[1] and Lengauer et al.[6] studies, respectively. The specific heat capacity of TiC–SiC composites was calculated using the law of mixture.

## 3. Results and discussion

### 3.1. Process optimisation

#### 3.1.1. Chemical analysis

Fig. 1 reports the X-ray diffraction patterns of TiC–SiC composites sintered at 1900 °C. Only two crystallized phases

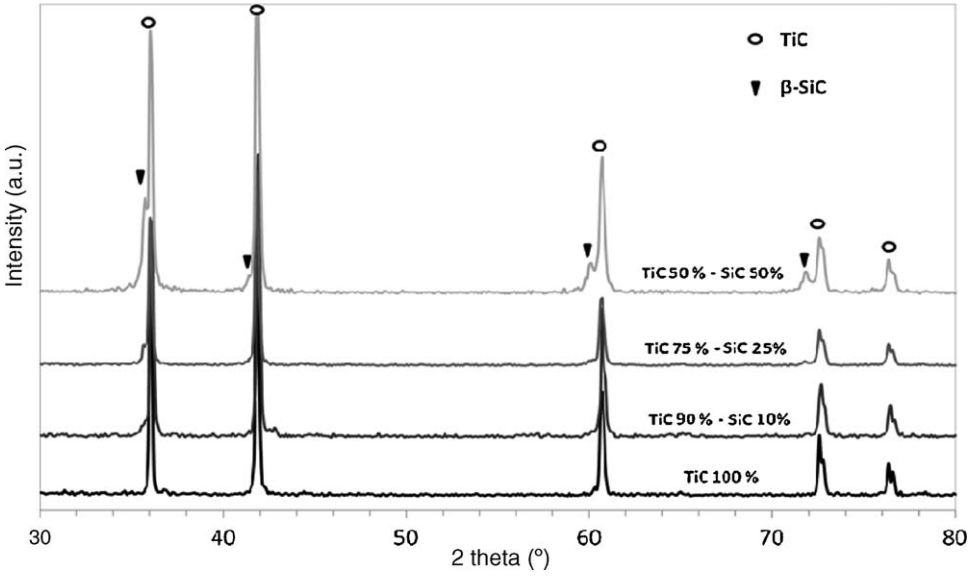


Fig. 1. XRD patterns of the TiC–SiC composites sintered at 1900 °C for 10 min.

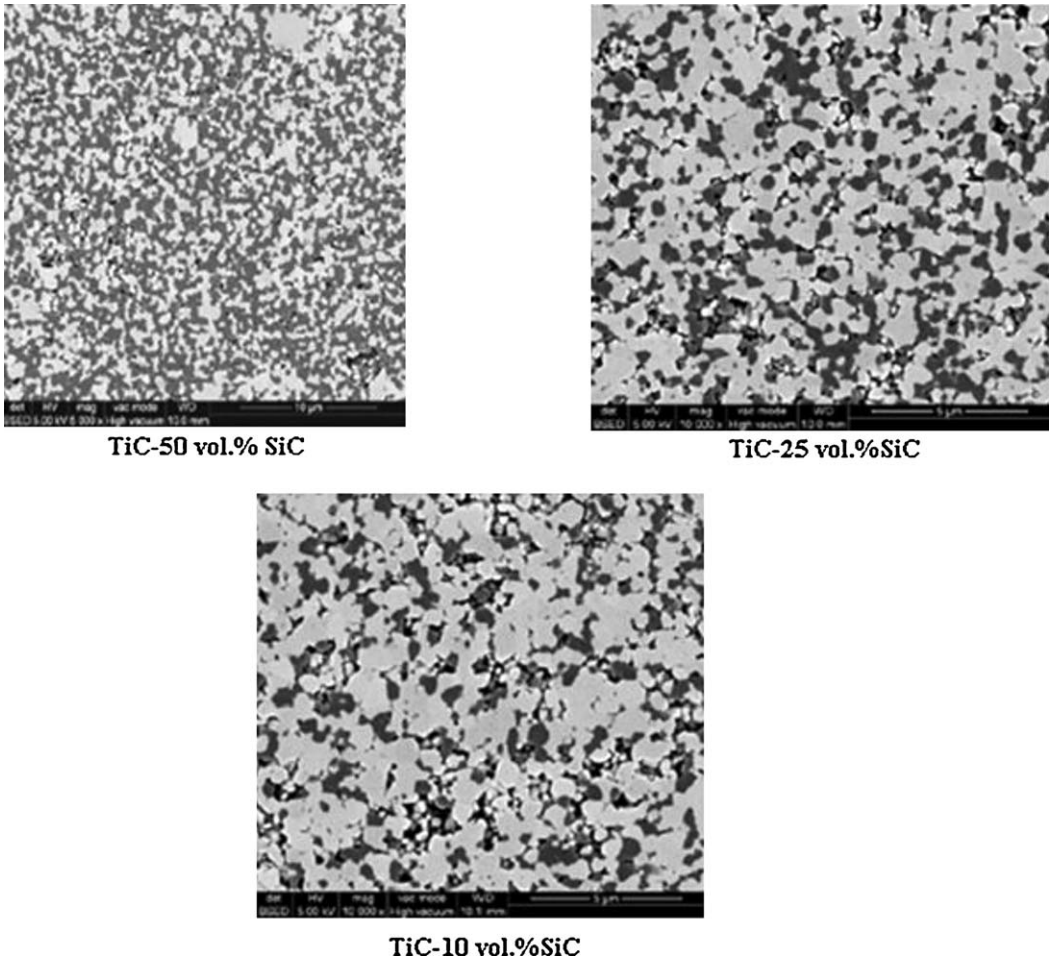


Fig. 2. SiC distribution in TiC–SiC samples sintered by SPS at 1800 °C for 10 min (SiC as dark phase).

are detected, respectively TiC and SiC for all samples (from TiC–50 vol.% SiC to TiC–10 vol.% SiC). As both TiC and SiC are cubic, the diffraction peaks of SiC and TiC are very close.

EPMA analyses of specimens sintered at 1900 °C are presented in Table 2. TiC–SiC ratio is near from the one expected. It is then possible to estimate the theoretical density of the samples by using law of mixture, with a density of 3.2 and 4.9, respectively for pure SiC and TiC.

XRD and EMPA analyses reveal no evidence of reaction between TiC and SiC during sintering. This observation is consistent with the various studies on the binary system TiC–SiC which indicate no solid solution.[9,11,12] Finally, it appears that SiC is well distributed into TiC and seems to prevent the TiC grains growth (Fig. 2).

Table 2
SiC and TiC contents in the as sintered samples.

| | Expected SiC volume content | | | |
|---|---|---|---|---|
| | 50% | 25% | 10% | 0% |
| TiC vol.% | 55 ± 1 | 78 ± 1 | 91 ± 1 | 100 |
| SiC vol.% | 45 ± 1 | 22 ± 1 | 9 ± 1 | 0 |
| Theoretical density | 4.1 ± 0.2 | 4.5 ± 0.2 | 4.8 ± 0.2 | 4.9 |

### 3.1.2. Temperature selection

Relative density has been calculated using theoretical density presented in Table 2. The evolution of density as a function of temperature and composition is reported in Fig. 3. The density increases with temperature: the maximal density is reached for a sintering temperature of 1900 °C (between 96 and 98% for the whole compositions). The density of samples sintered at 1700 °C

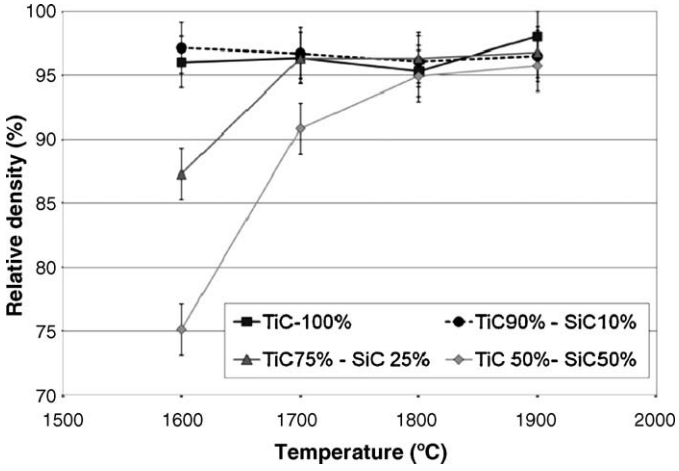


Fig. 3. Evolution of relative density according to temperature and composition.

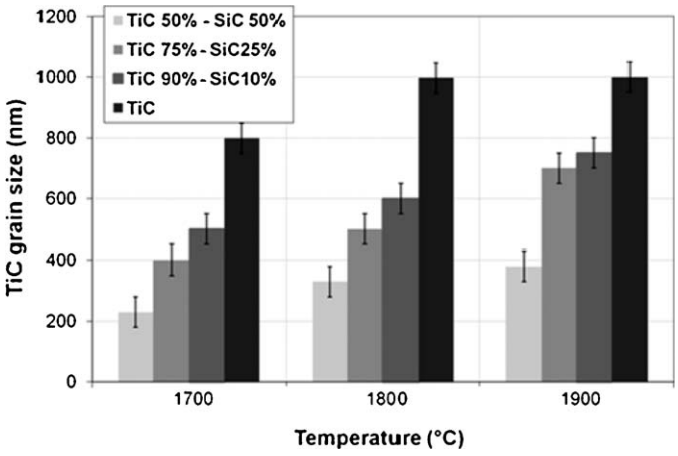


Fig. 4. TiC grain size of TiC–SiC composites with different SiC volume contents, and for several sintering temperatures.

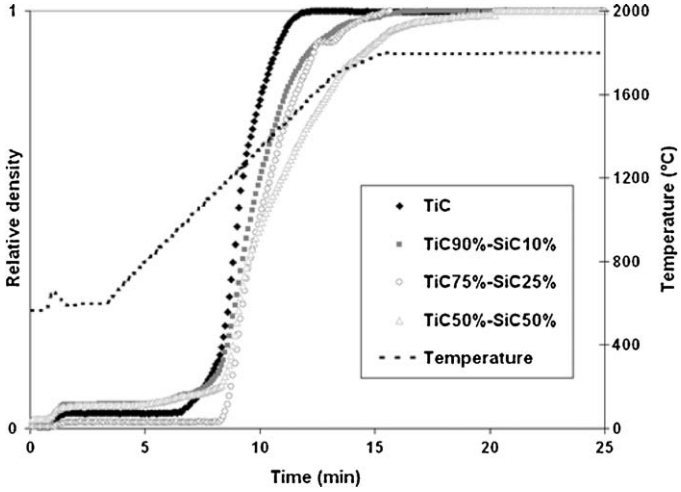


Fig. 5. Dilatometric curves of samples sintered at 1800 °C, with holding time of 10 min.

and 1600 °C is lower, especially for samples containing large SiC ratio. Sintering temperatures of 1600 °C and 1700 °C are not high enough to achieve a density higher than 95% for all compositions. Indeed, density ranges from 75% (50% SiC) to 97% (TiC) at 1600 °C and from 91% (50% SiC) to 97% (TiC) at 1700 °C. Thus, it appears that with a pressure of 50 MPa, a sintering temperature at least equal at 1800 °C is necessary to reach a minimum density of 95%, whatever TiC–SiC composites composition considered.

Fig. 4 presents the evolution of the grain size as a function of composition for several sintering temperatures. Whatever the temperatures, add of SiC allows reducing TiC grain size. However, the higher the temperature is, the higher the samples grain size is.

Thus, it is clear that to minimize porosity and grain coarsening at the same time, the sintering temperature selected is 1800 °C.

### 3.1.3. Pressure and holding time

A sintering temperature of 1800 °C has been selected to fabricate dense TiC–SiC composites, with small grain size and low porosity. However, and as shown in Fig. 5, it seems that holding time of 10 min is too long. Indeed, dilatometric curves indicate that for samples containing less than 50%, the maximal density was reached before the final sintering temperature was reached. For a SiC ratio of 50%, the density keep on increasing during the holding time at 1800 °C.

It should be possible to reduce grain coarsening, and to keep a low porosity by reducing holding time from 10 to 5 min. In the same time, in order to minimize porosity, pressure is increased from 50 MPa to 75 MPa. As reported in Table 3, the increase of pressure leads to a decrease of porosity, whereas reduction of sintering time induces a decrease of grain coarsening.

As shown in Fig. 6, SiC grains are located on TiC grain boundaries and seem to inhibit the growth of TiC grains. The grain size of TiC is strongly decreased by moving SiC ratio from 0 vol.% to 50 vol.% (Fig. 6d). It is also interesting to note that the growth of SiC grains does not significantly increase with the increasing of SiC ratio and that the evolution of dilatometric curves for different SiC contents indicate that SiC-poor samples reach faster their maximal relative density.

All those observations are in a good agreement with the literature which indicate a less effective sintering of SiC than TiC in this range of temperature and pressure.[13] Indeed, improved SPS temperature of SiC is 1850 °C and enables to obtain a density around 90%.[14] So under 1800 °C, the temperature selected in this study, SiC is not completely dense, contrary to TiC which can be sintered at lower temperature (from 1600 °C).[8] The samples sintered for 5 min at 1800 °C and under a pressure of 75 MPa have been characterized more thoroughly, in term of mechanical and thermal behaviour.

## 3.2. Mechanical properties

Fig. 7 presents the relationship between the Vickers hardness and SiC contents. The Vickers hardness of TiC–SiC composites sintered at 1800 °C exhibits a slight increase with the increment of SiC volume content. Those composites have a similar den-

Table 3
Density and grain size of samples sintered at 1800 °C: effect of pressure and holding time.

| | TiC | TiC–10 vol.% SiC | TiC–25 vol.% SiC | TiC–50 vol.% SiC |
|---|---|---|---|---|
| Relative density (%) | | | | |
| 10 min 50 MPa | 94.9 | 96.3 | 96.1 | 95.3 |
| 5 min 75 MPa | 95.4 | 97.2 | 97.3 | 97.3 |
| TiC grain size (nm) | | | | |
| 10 min 50 MPa | 1000 | 700 | 500 | 330 |
| 5 min 75 MPa | 900 | 540 | 400 | 270 |

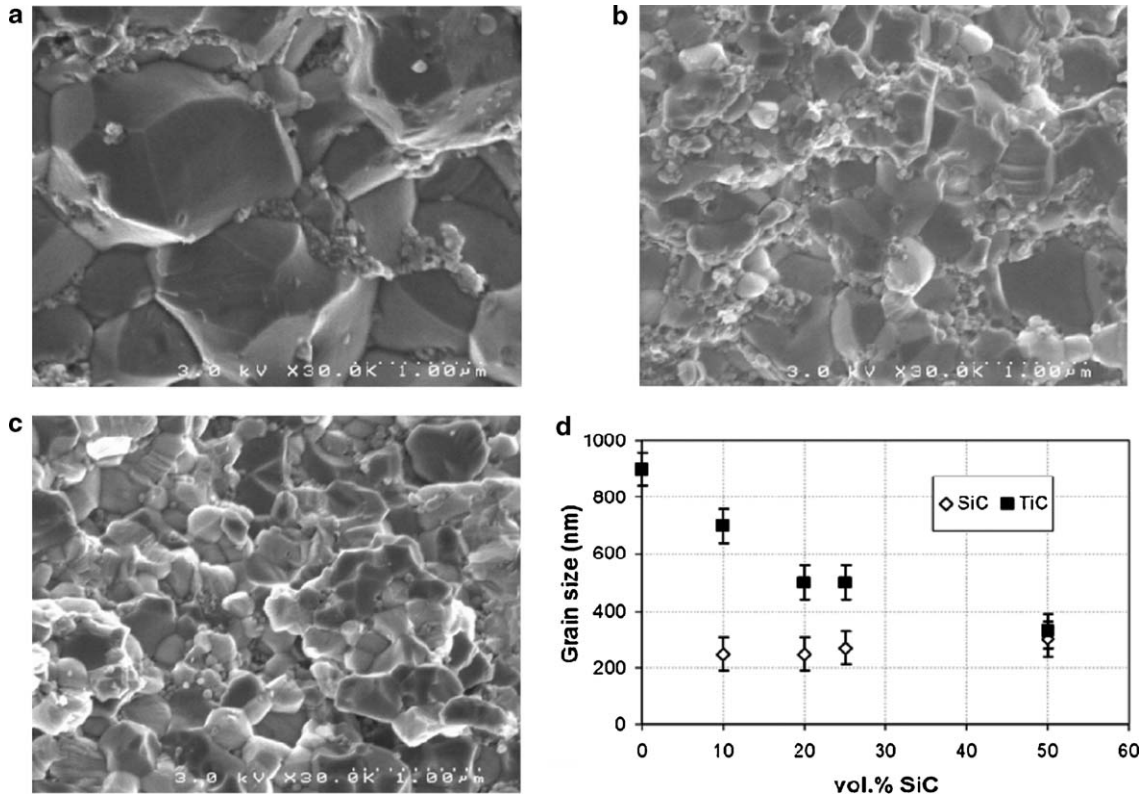


Fig. 6. SEM images of the fracture surfaces of TiC–SiC composites sintered at 1800 °C. (a) 0 vol.%, (b) 25 vol.%, (c) 50 vol.% and (d) grain size of TiC and SiC in several TiC–SiC composites sintered at 1800 °C for 5 min and under 75 MPa.

sity, thus, we can conclude that increase of Vickers hardness is associated to SiC volume content, and that SiC is harder than TiC.[15] As a comparison, the specimens sintered at 1600 °C and 1700 °C exhibit a decrease of Vickers hardness as a function of SiC ratio because density of these composites decreases with SiC ratio. An assessment of fracture toughness can be calculated from indentation test. Under sharp indenters, two distinguished types of cracks are usually formed: shallow, surface cracks (also referred to as Palmquist-cracks) emerging from the corners of the hardness impression, and half penny cracks. To distinguish between these two crack systems, a formal criterion based on the crack-length/indent diagonal ratio was proposed.[16] Examination of cracks shape indicates that they are Palmquist cracks ($0.25 \leq l/a \leq 2.5$). For such cracks, Niihara derived the following equation for fracture toughness determined from Vickers indentation[16]:

$$K_{IC} = 0.0089 \times \left(\frac{E}{H_v}\right)^{2/5} \times \frac{P}{a \times l^{1/2}}$$

where $E$ is the Young modulus (Pa) taken from the literature[16] (the law of mixture was applied for TiC–SiC composites), $H_v$ is the Vickers hardness (Pa) $P$ is the applied load (N), $2a$ is diagonal length of the Vickers indents mark and $l$ is the crack length. The fracture toughness ($K_{IC}$) of TiC–SiC composites reached maximum $K_{IC\,max} = 5.6\,MPa\,m^{1/2}$ when SiC content is up to 50%, whereas fracture toughness of pure TiC is about $3.7\,MPa\,m^{1/2}$ (Fig. 8). Thus, the fracture toughness can be enhanced by introducing a second phase in TiC. This is in a good agreement with several studies.[16–18]

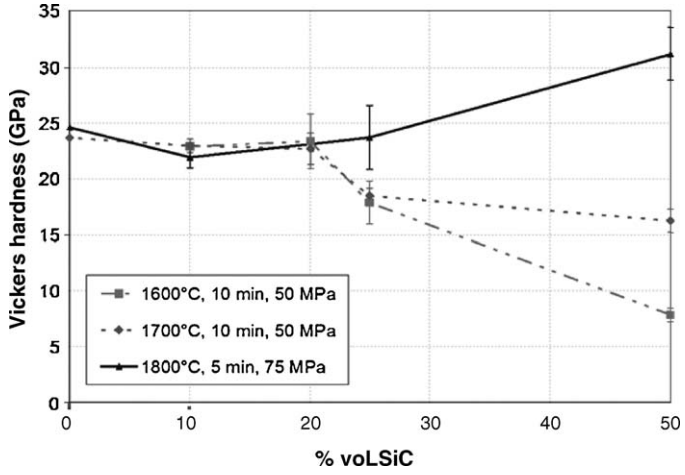


Fig. 7. The Vickers hardness of TiC–SiC composites with different SiC volume contents, and several sintering conditions.

The increase of fracture toughness can be attributed to the deflection of the cracks due to distribution of different particles as shown in Fig. 9.

Indeed, adding SiC presents two benefit effects on the microstructure of TiC–SiC composites.

- First, presence of SiC grains evidently prevents the coalescence of TiC grains (Figs. 6–8).

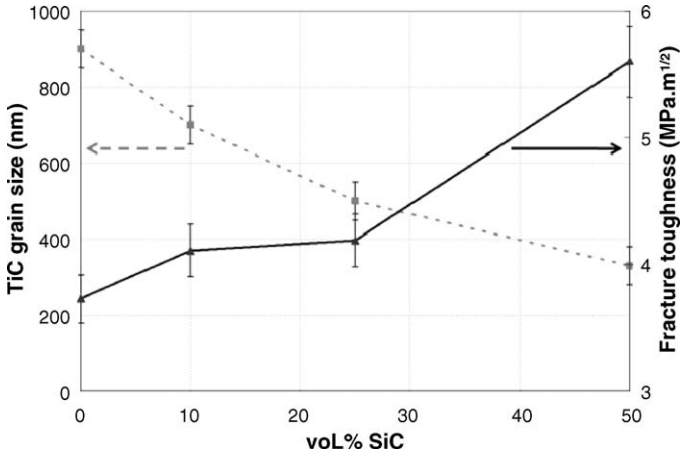


Fig. 8. Relationship between $K_{IC}$ and SiC content of TiC–SiC composites $T_{sintering} = 1800\,^{\circ}C$, $P = 75$ MPa, 5 min.

- Then, even after sintering, SiC grains keep a smaller size than TiC grains (Fig. 6d).

As a consequence, the introduction of nano-sized SiC leads to a finer microstructure. In such microstructure, the fracture mode is mostly intergranular. The observation of fracture surface indicates fine SiC grains located on the grain boundaries of coarse TiC grains. When the cracks propagate and reach a sub-micro-grains of TiC or SiC, it is difficult for the crack to cross through the particles, and the crack will deflect and propagate along the SiC and TiC grains boundaries as reported by Luo et al.[9] and Wang et al.[10] Others authors have also attributed the crack deflection to the residual stress generated by the difference in thermal expansion coefficient and elastic modulus between SiC and TiC.[18,19]

### 3.3. Thermal conductivity

The temperature dependence of the thermal conductivity of TiC–SiC composites with different SiC volume contents is shown in Fig. 10. As reported in the literature, thermal conductivity of TiC increases with temperature. This is characteristic of transition metal carbides and TiC in particular, where heat transfer is assumed by electrons rather than phonons.[6]

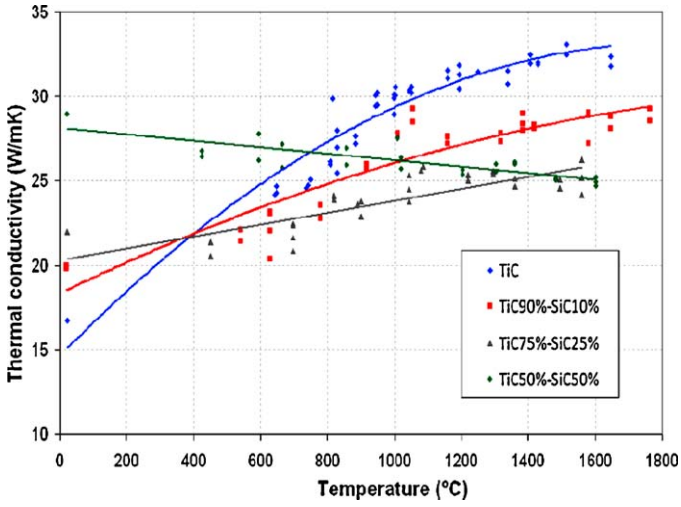


Fig. 10. Temperature dependence of thermal conductivity of TiC–SiC composites with various SiC volume contents (error bars no presented in the graph are determined at ±1 W/m K).

With the introduction of SiC two contradictory effects are observed. The fine microstructure associated to nano-sized SiC adding, with a higher grain boundaries concentration than in pure TiC samples, should lead to a lower thermal conductivity. However, as thermal conductivity of SiC is much higher than thermal conductivity of TiC at room temperature (17 W/m K for TiC, and 100 W/m K for SiC), the introduction of SiC could also lead to an increase of thermal conductivity of TiC–SiC composites. Here, thermal conductivity increases with the addition of SiC at room temperature (respectively 16.5 W/m K, 20 W/m K, 22 W/m K and 27 W/m K for TiC, TiC–10 vol.% SiC, TiC–25 vol.% SiC, TiC–50 vol.% SiC). We can deduce that the effect of the composition is dominant on the effect of the microstructure.

The thermal conductivity of TiC, TiC–10 vol.% SiC and TiC–25 vol.% SiC exhibits an increase trend as the temperature increases. This increase is higher for monolithic TiC than for composite. Due to the low volume fraction and random distribution of SiC, SiC grains cannot form a continuous paths through the matrix, thus, the thermal conductivity is mainly controlled by the TiC behaviour. As a conclusion, thermal conductivity of TiC–SiC increases with the rise of temperature, provided that the SiC volume content is minor to 25%. For a SiC ratio of 50%,

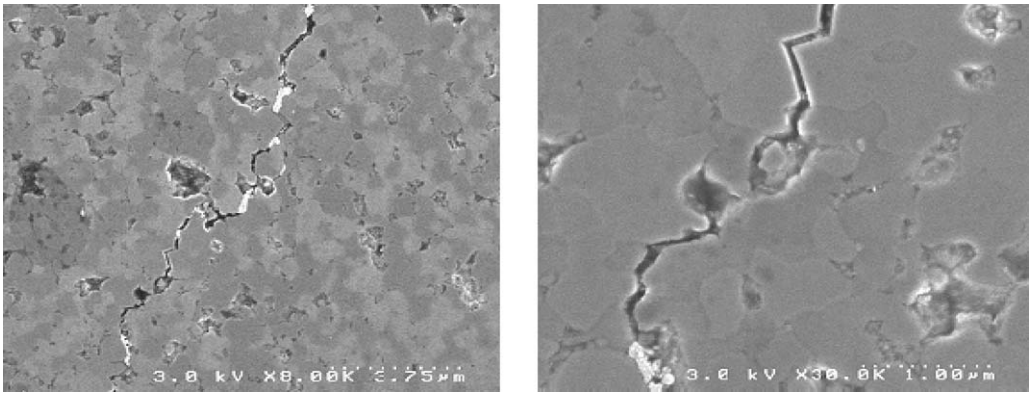

Fig. 9. SEM micrographs of crack paths induced by a Vickers indenter in TiC–50 vol.% SiC.

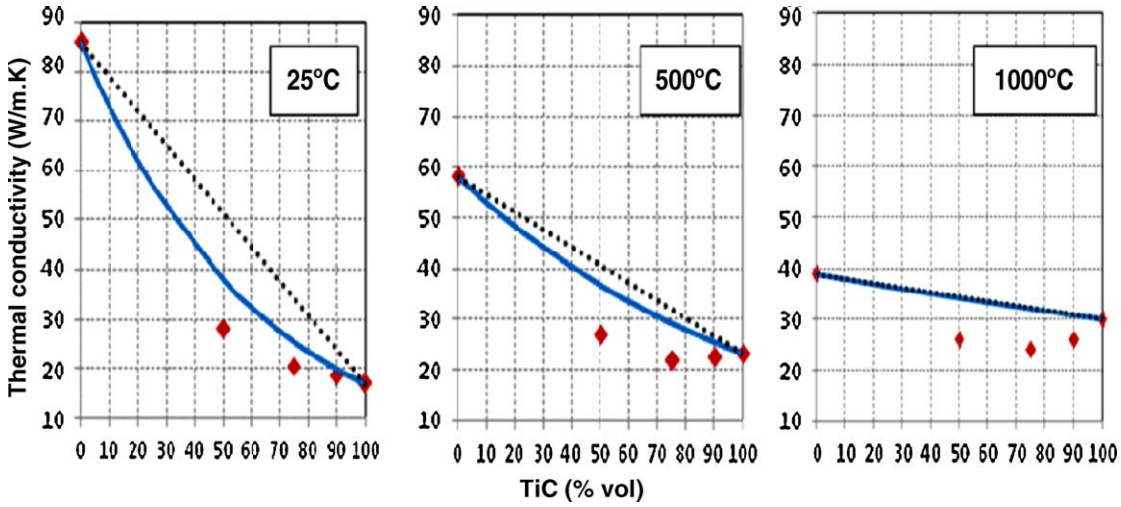


Fig. 11. Thermal conductivity as a function of composition. Point: experimental data; dashed line: arithmetic average; full line: geometric average.

thermal conductivity exhibits a slight decrease with the rise of the temperature. In this case, thermal behaviour is mainly associated to SiC behaviour. Due to those different behaviours, at 1600 °C, lower is the SiC ratio, higher is the thermal conductivity.

For a better understanding of the SiC ratio effect, and to verify if the low of mixtures could be applied to such compounds, pure SiC samples have been fabricated (same SiC, powder than for TiC–SiC composites, $P = 75$ MPa, $T = 1800$ °C for 5 min), and thermal conductivity has been measured for those materials at room temperature, 500 °C and 1000 °C, as shown in Fig. 11. It is then possible, for several temperatures to plot the thermal conductivity as a function of composition, from pure SiC to pure TiC.

Many models aim to forecast the thermal properties of two phases materials from the characteristics of each component and their volume fractions.[20] Limiting parameters are those linked to morphology, distribution and contact of the phases because they are quite uneasy to describe: independent spheres,[21] interconnected spheres,[22] geometric aspect ratio,[23] etc. Commonly, the experimental conductivity of a two-phase-material is reported as the arithmetic average (linear):

$$k_{\text{arithm.}} = k_1\Phi + k_2(1 - \Phi)$$

or the geometric average:

$$k_{\text{geom.}} = {k_1}^{\Phi}{k_2}^{(1-\Phi)}$$

with $k_1$ and $\Phi$ the conductivity and volume fraction of the dispersed phase and $k_2$ the matrix conductivity.[24] These two formulas were used to evaluate the thermal conductivity of the two-phase SiC–TiC, according to the following hypothesis:

- Thermal conductivity of each phase, TiC and SiC, in the composites is assimilated to the conductivity of single-phase TiC and SiC;
- Porosity is zero;
- Thermal resistance at interface is zero.

The experimental and calculated evolutions of conductivity versus the ceramic phase volume fraction are presented in Fig. 11 at 25 °C, 500 °C and 1000 °C.

Clearly, the experimental data do not follow the law of mixture. The calculations systematically over-estimate the experimental conductivity. As shown in microstructure observations, a lot of interfaces exist due to grain boundaries, and the thermal resistance effect cannot be neglected; among all the hypothesis, this could reasonably explain such a discrepancy. It is interesting to note that at 1000 °C, thermal conductivity of TiC–SiC composites are lower than thermal conductivity of pure SiC and TiC. This result could be explained by the different mechanisms which ensure thermal conductivity in TiC and in SiC at high temperature. In silicon carbide, heat transfer is assumed by phonons whereas it is assumed by electrons in titanium carbide. At high temperature, thermal conductivity of TiC (which increase with temperature due to electrons) is reduced with the addition of SiC because SiC grains act as thermal resistances, disturbing electrons displacement (SiC acts as an insulator). As a contrary, TiC in $TiC_{50\%}$–$SiC_{50\%}$ increases phonons diffusion and reduces thermal conductivity of TiC–SiC composites.

## 4. Conclusion

In the present paper, nano-sized TiC–SiC mixtures with 97% relative density were processed at 1800 °C without any sintering aids by spark plasma sintering. XRD and EDX analyses indicated that there is no reaction between SiC and TiC phases; the add of nano-sized SiC obviously hinders the coalescence of TiC grains, and thus increases the fracture toughness of the composite. Temperature dependence of thermal conductivity was investigated. Two domains have been highlighted: when SiC volume content is at least smaller than 25%, TiC–SiC composite exhibits titanium carbide like behaviour. Thermal conductivity increases with the rise of temperature. When SiC volume content is at least higher than 50%, TiC–SiC composite exhibits a silicon carbide like behaviour:

the thermal conductivity decreases with the rise of temperature.

Those materials will be irradiated using heavy ions to simulate neutron irradiation. It will be then possible to study the irradiation effect on thermal conductivity, and that according to both composition and microstructure.

## Acknowledgements

This study was financially supported by French Research Group MATINEX. The authors would thank J. Galy and C. Estournes for allowing us to use spark plasma sintering, M. Lahaye, from Cecama, ICMCB, Pessac for carrying out the X-ray microprobe analyses and C. Richaud from CEA for thermal conductivity measurements.

## References

1. Snead LL, Nozawa T, Katoh Y, Byun TS, Kondo S, Petti DA. Handbook of SiC properties for fuel performance modelling. *J Nucl Mater* 2007;**371**:329–77.
2. Naslain R, Christin F. SiC-matrix composite materials for advanced jet engines. *MRS Bull* 2003:654–8.
3. Maruyama T, Harayama M. Relationship between dimensional changes and the thermal conductivity of neutron irradiated SiC. *J Nucl Mater* 2004;**329–333**:1022–8.
4. Akiyoshi M, Takagi I, Yano T, Akasaka N, Tachi Y. Thermal conductivity of ceramics during irradiation. *Fusion Eng Des* 2006;**81**:321–5.
5. Senor DJ, Youngblood GE, Greenwood LR, Archer DV, Alexander DL, Chen MC, et al. Defect structure and evolution in silicon carbide irradiated to 1 dpa-SiC at 1100 °C. *J Nucl Mater* 2003;**317**:145–59.
6. Lengauer W, Binder S, Aigner K. Solid state properties of group IVb carbonitrides. *J Alloys Compd* 1995;**217**:137–47.
7. Smith ER, Johnson D, Brockway C, Thompson JK, Lynch JF. Engineering property data of selected ceramics. Carbides MCIC Report, vol. 2; 1979.
8. Wang L, Jiang W, Chen L. Fabrication of nano SiC particles reinforced TiC/SiC nano composites. *Mater Lett* 2004;**58**:1401–4.
9. Luo Y, Li S, Pan W, Li L. Fabrication and mechanical evaluation of SiC–TiC nanocomposite by SPS. *Mater Lett* 2003;**58**:150–3.
10. Wang L, Jiang W, Chen L. Rapidly sintering nanosized SiC particle reinforced TiC composites by the spark plasma sintering (SPS) technique. *J Mater Sci* 2004;**39**:4515–9.
11. Liversage JH, McLachlan SD, Sigalas I. Microstructure, phase and thermoelastic properties of laminated liquid-phase-sintered silicon carbide–titanium carbide ceramic composites. *J Am Ceram Soc* 2007;**90**:2189–95.
12. An HG, Kim YW, Lee JG. Effect of initial α-phase content of SiC on microstructure and mechanical properties of SIC–TiC composite. *J Eur Ceram Soc* 2001;**21**:93–8.
13. Maitre A, Vande Put A, Laval JP, Trolliard G. Role of boron on the spark plasma sintering of an α-SiC powder. *J Eur Ceram Soc* 2008;**28**:1881–90.
14. Guillard F, Allemand A, Lulewicz JD, Galy J. Densification of SiC by SPS-effects of time, temperature and pressure. *J Eur Ceram Soc* 2007;**27**:2725–8.
15. Chen J, Li WJ, Jiang W. Characterization of sintered TiC–SiC composites. *Ceram Int* 2009;**35**:3125–9.
16. Niihara K, Morena R, Hasselman DPH. Evaluation of the $K_{IC}$ of brittle solids by the indentation method with low crack-to-indent ratios. *J Mater Sci Lett* 1982:13–6.
17. Endo H, Ueki M, Kubo H. Microstructure and mechanical properties of hot pressed SiC–TiC composites. *J Mater Sci* 1991;**26**:3769–74.
18. Cho KS, Kim YW, Choi HJ, Lee JG. In situ toughened silicon carbide–titanium carbide composites. *J Am Ceram Soc* 1996;**79**:1711–3.
19. Evans AG, Langdon TG. Structural ceramics. *Prog Mater Sci* 1976;**21**:171.
20. Belova IV, Murch GE. Monte Carlo simulation of the effective thermal conductivity in two-phase material. *J Mater Proc Technol* 2004;**153–154**:741.
21. Maxwell JC. *Treatise on Electricity and Magnetism*, vol. 1. Clarendon: Oxford; 1982.
22. Singh KJ, Singh R, Chaudhary DR. Heat conduction and a porosity correction term for spherical and cubic particles in a simple cubic packing. *J Phys D: Appl Phys* 1998;**31**:1681.
23. Verma LS, Shrotriya AK, Singh R, Chaudhary DR. Thermal conduction in two-phase materials with spherical and nonspherical inclusions. *J Phys D: Appl Phys* 1991;**24**:1729.
24. Le Flem M, Allemand A, Urvoy S, Cédat D, Rey C. Microstructure and thermal conductivity of Mo–TiC cermets processed by hot isostatic pressing. *J Nucl Mater* 2008;**380**:85–92.